Supporting Information

Quantitative Analysis of the Molecular Dynamics of P3HT:PCBM Bulk Heterojunction

Anne A. Y. Guilbert[1*], *Mohamed Zbiri*[2**], *Alan D.F. Dunbar*[3], *Jenny Nelson*[1]

[1] Centre for Plastic Electronics and Department of Physics, Blackett Laboratory, Imperial College London, London SW7 2AZ, United Kingdom.

[2] Institut Laue-Langevin, 71 avenue des Martyrs, Grenoble Cedex 9, 38042, France.

[3] Department of Chemical and Biological Engineering, the University of Sheffield, Sheffield S1 3JD, United Kingdom.

MOLECULAR DYNAMICS

We used the P3HT force field developed by Moreno *et al.*[1] for the amorphous simulations of h-P3HT and its blend with PCBM. We modified the inter-monomer dihedral potential following the potential proposed by Darling *et al.*[2] We calculated the potential energy surface of this dihedral for an oligomer of 14mers length using MP2/cc-pVTZ and integrated it in the force field by subtracting the potential energy surface from the force field with the dihedral of interest switched off. The parameters are as follow (using the following convention $V(\varphi) = \sum_{n=0}^{5} C_n cos^n(\varphi - 180°)$):

C_0	C_1	C_2	C_3	C_4	C_5
24.0 kJ.mol^{-1}	-0.6 kJ.mol^{-1}	-21.8 kJ.mol^{-1}	3.2 kJ.mol^{-1}	-5.0 kJ.mol^{-1}	-2.8 kJ.mol^{-1}

For PCBM, we used the force field developed by Cheung *et al.*[3] For d-P3HT and d-PCBM, we changed the mass of the hydrogen atom (1.008 u) to the mass of deuterium (2.014 u).

MD simulations were performed using Gromacs-4.6.5 package,[4–6] where a leapfrog algorithm was adopted. Periodic boundary conditions are applied in all directions. First, we relaxed the structure through energy minimisation using the steepest descent algorithm. The convergence criterion was set such that the maximum force is smaller than 10 kJ.mol^{-1}.nm^{-1}. This was followed by a run in the NVT ensemble for 100 ps in order to initially stabilise the temperature, followed by a 10 ns run in the NPT ensemble in order to stabilise the pressure this time. Depending on the ensemble NVT or NPT, we used a velocity-rescaling thermostat[7] (varying temperature, time constant 0.1 ps) and a Berendsen barostat (1 bar, compressibility 4.5.10^{-5} bar^{-1}, time constant 5 ps), respectively.

For the amorphous samples, 20mers of P3HT were used and packed randomly with or without PCBM in boxes using Packmol.[8] We first started by creating a melt at 600K by stabilizing both temperature and pressure. The size of the final box was checked to be larger than the length of an elongated 20mers of P3HT (7.3 nm) plus the cut-off radius used for the van der Waals forces (1.2 nm). The next step was to cool down the box, in the NPT ensemble, from the obtained NPT equilibrium phase at 600 K at a rate of -45K/ns by step of 50K. Every 50K, a full equilibration was again carried out. We followed the same protocol as in our previous paper, where the glass transition of P3HT was reproduced.[9] The density as function of temperature is plotted for amorphous P3HT, PCBM and the amorphous mixture of P3HT:PCBM (blend). All these steps were performed with a time step of 1fs.

The simulation lengths (50 ns) are chosen to be much longer than the experimental time windows (50 ps) in order to increase statistics and capture the impact of the slower relaxations on the faster motions. For these acquisition runs, we used a time step of 2fs (the bonds with hydrogen atoms were constrained), the Particle-mesh Ewald (PME) method for the electrostatic, the velocity-rescaling thermostat (varying temperature, time constant 0.1 ps) and a Berendsen barostat (1 bar, compressibility $4.5.10^{-5}$ bar^{-1}, time constant 5 ps), We note that in a previous work on P3HT,[9] we did not find any discrepancies between the simulations done using the more accurate Nose-Hoover thermostat and the velocity-rescaling thermostat.

For the crystalline samples, P3HT and PCBM were packed in a space group $P2_1/c$[10] and $P2_1/n$[11] respectively. Lots of different crystal structures are reported in the literature. We chose one for the purpose of illustrating the difference in relaxation times between an ordered and disordered sample, thus the actual crystal structure does not matter too much.

The conformational entropy was calculated by first building and diagonalising the covariance matrix of the atomic fluctuations and then using the Schlitter formula.[12]

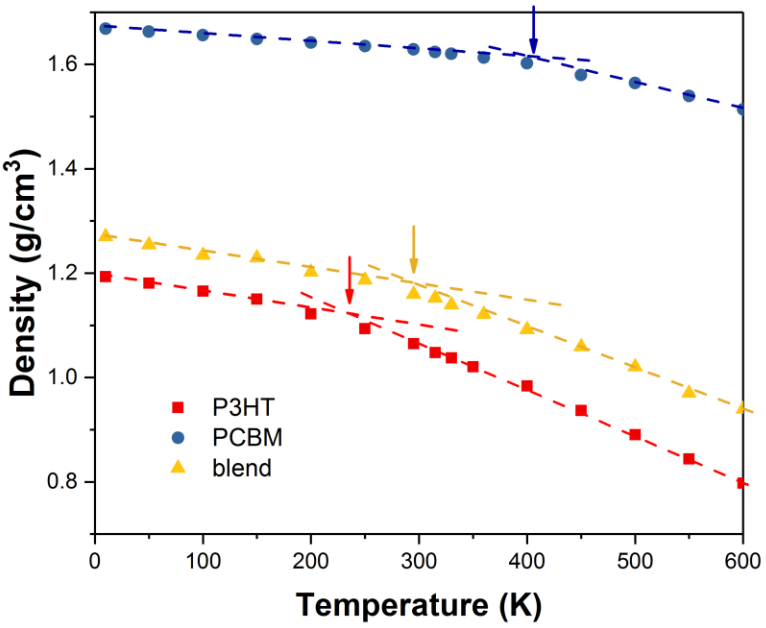

Figure S1. Density as a function of P3HT, PCBM and the amorphous mixture of P3HT:PCBM. The arrows indicate the glass transition.

AUTOCORRELATION FUNCTIONS AND RELAXATION TIMES

The dihedral autocorrelation function DACF(t) can be described by Lipari-Szabo model:[13]

$$DACF(t) = (1 - S_D^2) * ACF(t) + S_D^2$$

where t denotes the time, S_D^2 is the dihedral order parameter and ACF(t) is the function shown in Figure S1. The order parameter S_D^2 were calculated from the dihedral distribution p(θ) using the following equation:[14]

$$S_D^2 = \left[\int_0^{2\pi} cos(\theta)p(\theta)d\theta\right]^2 + \left[\int_0^{2\pi} sin(\theta)p(\theta)d\theta\right]^2$$

The relaxation times (τ) were extracted from $ACF(t)$ assuming that $ACF(t)$ displays a stretched exponential behavior ($ACF(\tau) = e^{-1}$). We then calculated the probability distribution functions $P(E, \tau, \beta)$ using the equations described by Berberan-Santos *et al.*[15] We used the stretched exponent extracted from the experimental data.[16]

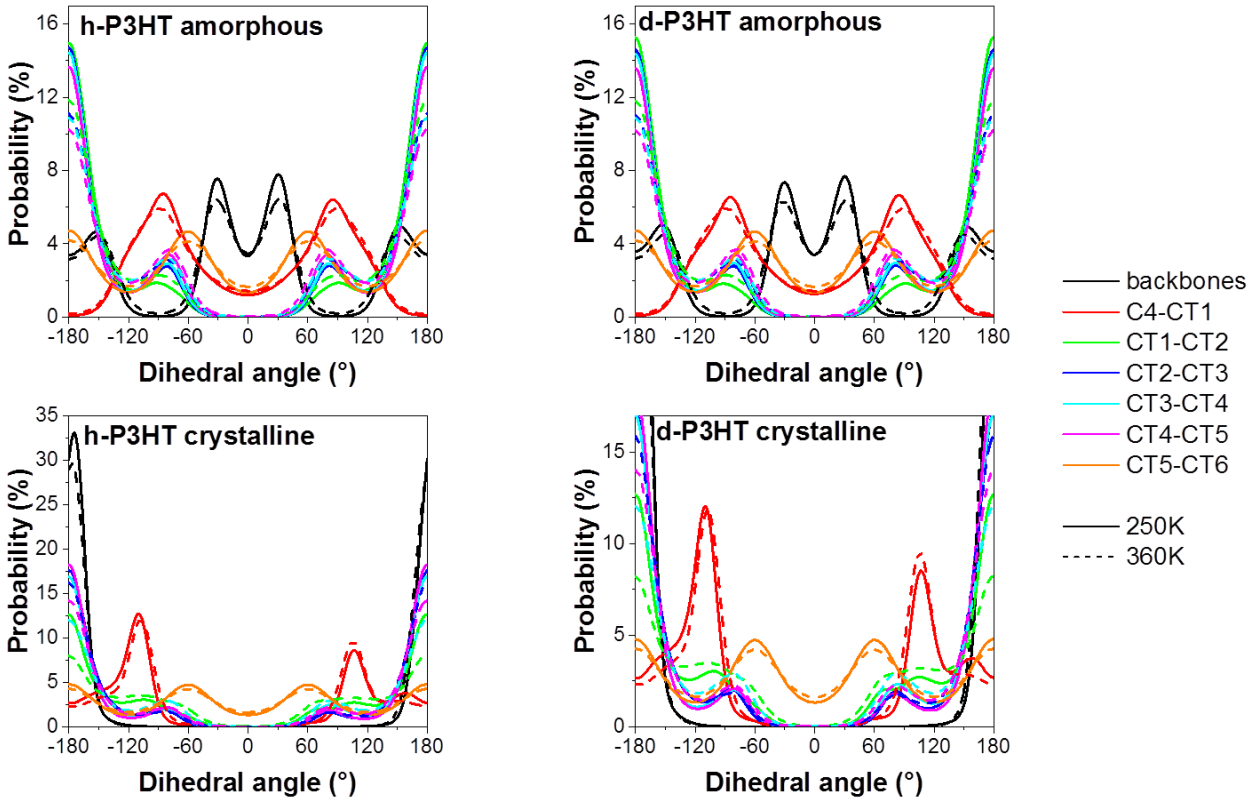

Figure S2. Dihedral distribution of the different degrees of freedom of amorphous and crystalline h-P3HT and d-P3HT.

Table S1. Dihedral parameter S_D^2 of the different degrees of freedom of amorphous and crystalline h-P3HT and d-P3HT.

	h-P3HT				d-P3HT			
	amorphous		crystalline		amorphous		crystalline	
	250K	360K	250K	360K	250K	360K	250K	360K
backbone	0.018	0.012	0.946	0.941	0.013	0.010	0.942	0.939
C4-CT1	0.012	0.009	0.251	0.188	0.014	0.009	0.247	0.185
CT1-CT2	0.536	0.416	0.375	0.209	0.546	0.415	0.372	0.218
CT2-CT3	0.448	0.333	0.591	0.563	0.445	0.331	0.566	0.540
CT3-CT4	0.425	0.318	0.523	0.359	0.421	0.317	0.529	0.362
CT4-CT5	0.364	0.258	0.563	0.473	0.361	0.257	0.568	0.460
CT5-CT6	0.000	0.000	0.000	0.000	0.000	0.000	0.000	0.000

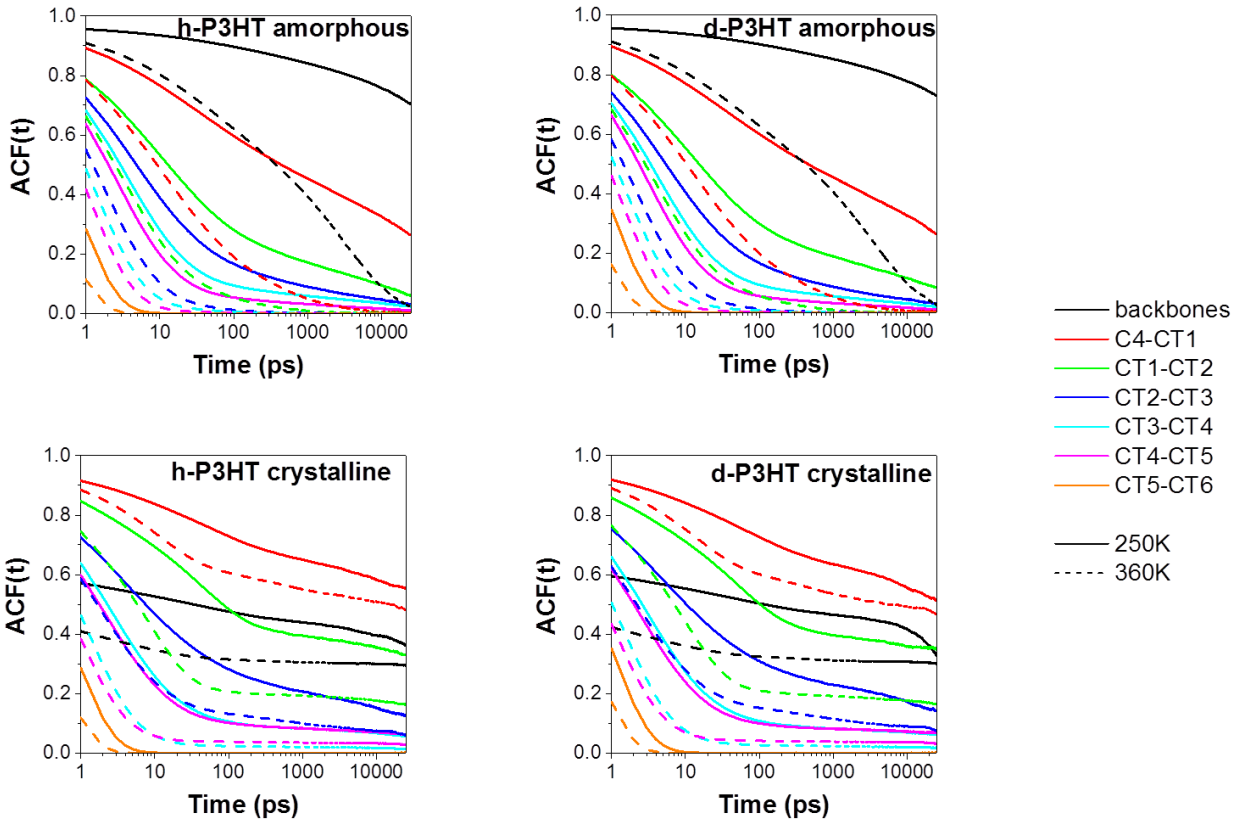

Figure S3. Autocorrelation functions of the different degrees of freedom of amorphous and crystalline h-P3HT and d-P3HT. The autocorrelation functions have been corrected for the stiffness of the degrees of freedom using S_D^2.

Table S2. Relaxation times of the different degrees of freedom of amorphous and crystalline h-P3HT and d-P3HT.

	h-P3HT				d-P3HT			
	amorphous		crystalline		amorphous		crystalline	
	250K	360K	250K	360K	250K	360K	250K	360K
backbone	_	1222 ps	_	_	_	1357 ps	_	_
C4-CT1	4751 ps	23 ps	_	_	4801 ps	25 ps	_	_
CT1-CT2	40 ps	5 ps	4906 ps	13 ps	47 ps	6 ps	6622 ps	16 ps
CT2-CT3	12 ps	3 ps	28 ps	4 ps	13 ps	3 ps	42 ps	5 ps
CT3-CT4	6 ps	2 ps	5 ps	3 ps	7 ps	2 ps	6 ps	2 ps
CT4-CT5	5 ps	< 1 ps	4 ps	1 ps	5 ps	2 ps	5 ps	2 ps
CT5-CT6	< 1 ps	< 1 ps	< 1 ps	< 1 ps	< 1 ps	< 1 ps	< 1 ps	< 1 ps

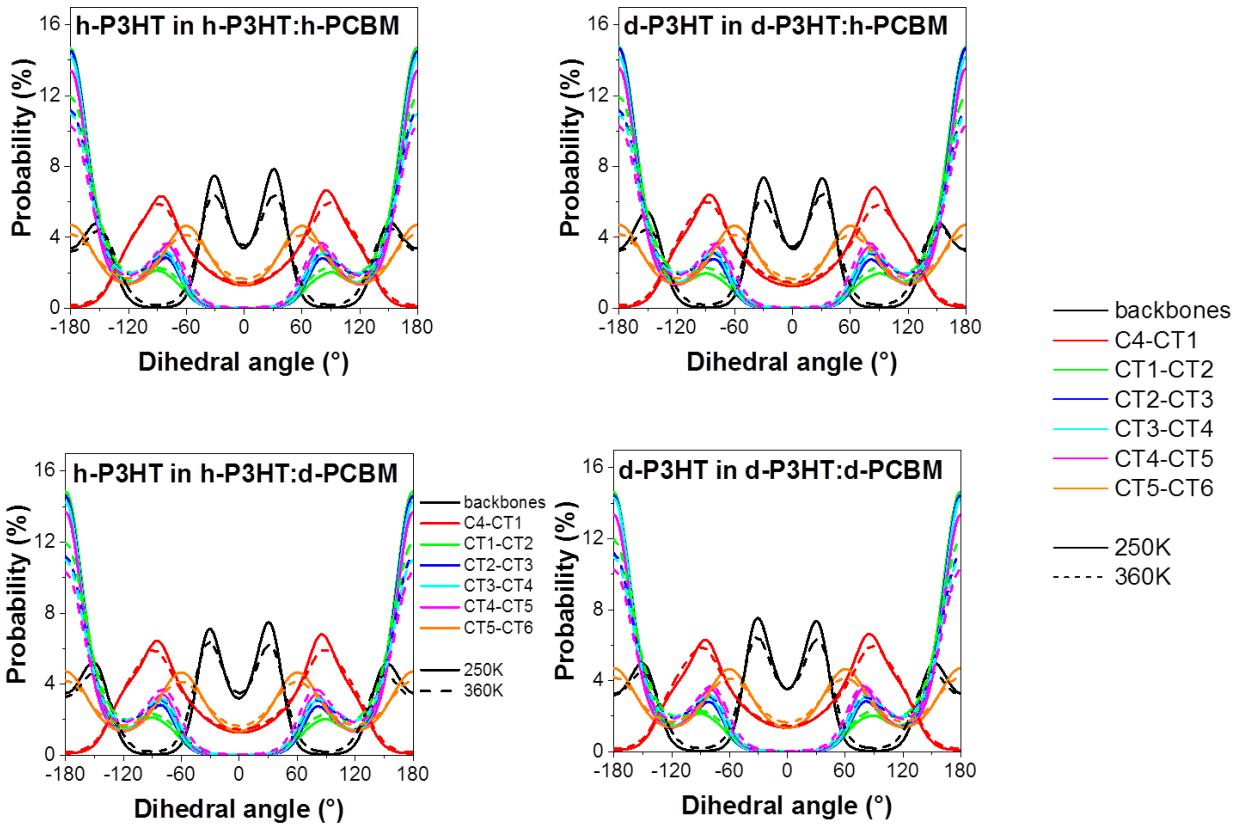

Figure S4. Dihedral distribution of the different degrees of freedom of h-P3HT and d-P3HT blended with h-PCBM and d-PCBM.

Table S3. Dihedral parameter S_D^2 of the different degrees of freedom of h-P3HT and d-P3HT blended with h-PCBM and d-PCBM.

	h-P3HT				d-P3HT			
in	h-P3HT:h-PCBM		h-P3HT:d-PCBM		d-P3HT:h-PCBM		d-P3HT:d-PCBM	
	250K	360K	250K	360K	250K	360K	250K	360K
backbone	0.019	0.011	0.007	0.008	0.011	0.009	0.015	0.011
C4-CT1	0.012	0.010	0.012	0.010	0.011	0.010	0.015	0.010
CT1-CT2	0.504	0.418	0.504	0.419	0.511	0.419	0.498	0.417
CT2-CT3	0.438	0.336	0.444	0.336	0.447	0.335	0.439	0.336
CT3-CT4	0.410	0.319	0.411	0.320	0.409	0.318	0.413	0.319
CT4-CT5	0.350	0.258	0.365	0.258	0.357	0.258	0.349	0.258
CT5-CT6	0.000	0.000	0.000	0.000	0.000	0.000	0.000	0.000

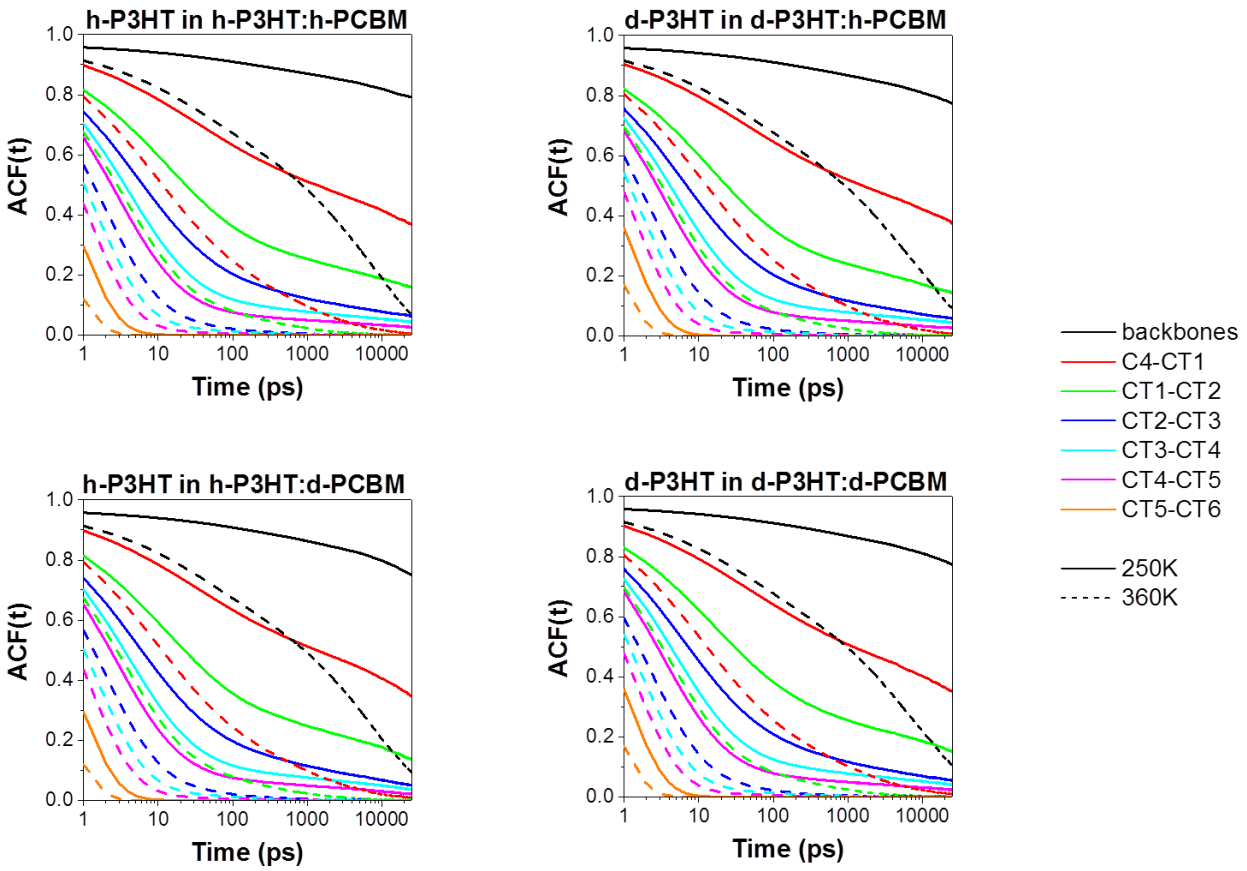

Figure S5. Autocorrelation functions of the different degrees of freedom of h-P3HT and d-P3HT blended with h-PCBM and d-PCBM. The autocorrelation functions have been corrected for the stiffness of the degrees of freedom using S_D^2.

Table S4. Relaxation times of the different degrees of freedom of h-P3HT and d-P3HT blended with h-PCBM and d-PCBM.

	h-P3HT				d-P3HT			
in	h-P3HT:h-PCBM		h-P3HT:d-PCBM		d-P3HT:h-PCBM		d-P3HT:d-PCBM	
	250K	360K	250K	360K	250K	360K	250K	360K
backbone	_	2712 ps	_	3081 ps	_	2962 ps	_	3162 ps
C4-CT1	24531 ps	31 ps	18424 ps	31 ps	_	34 ps	18403 ps	35 ps
CT1-CT2	80 ps	6 ps	86 ps	6 ps	84 ps	7 ps	120 ps	7 ps
CT2-CT3	17 ps	3 ps	15 ps	3 ps	18 ps	3 ps	19 ps	3 ps
CT3-CT4	7 ps	2 ps	7 ps	2 ps	8 ps	3 ps	9 ps	3 ps
CT4-CT5	5 ps	2 ps	5 ps	2 ps	6 ps	2 ps	6 ps	2 ps
CT5-CT6	< 1 ps	< 1 ps	< 1 ps	< 1 ps	< 1 ps	< 1 ps	< 1 ps	< 1 ps

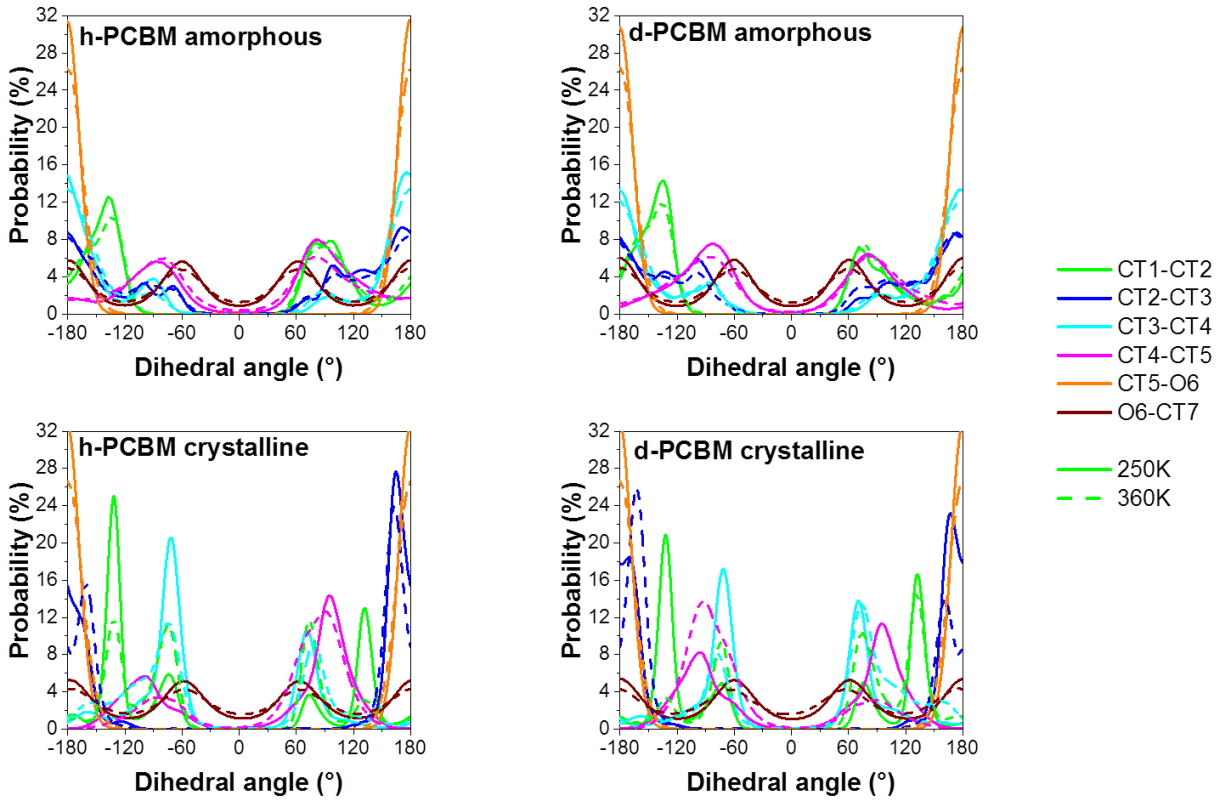

Figure S6. Dihedral distribution of the different degrees of freedom of amorphous and crystalline h-PCBM and d-PCBM.

Table S5. Dihedral parameter S_D^2 of the different degrees of freedom of amorphous and crystalline h-PCBM and d-PCBM.

	h-PCBM				d-PCBM			
	amorphous		crystalline		amorphous		crytalline	
	250K	360K	250K	360K	250K	360K	250K	360K
CT1-CT2	0.240	0.246	0.254	0.063	0.254	0.244	0.201	0.120
CT2-CT3	0.337	0.307	0.891	0.856	0.332	0.308	0.898	0.861
CT3-CT4	0.561	0.550	0.107	0.050	0.487	0.485	0.025	0.090
CT4-CT5	0.028	0.004	0.096	0.242	0.008	0.007	0.014	0.282
CT5-O6	0.950	0.929	0.953	0.930	0.950	0.929	0.953	0.930
O6-CT7	0.000	0.000	0.000	0.000	0.000	0.000	0.000	0.000

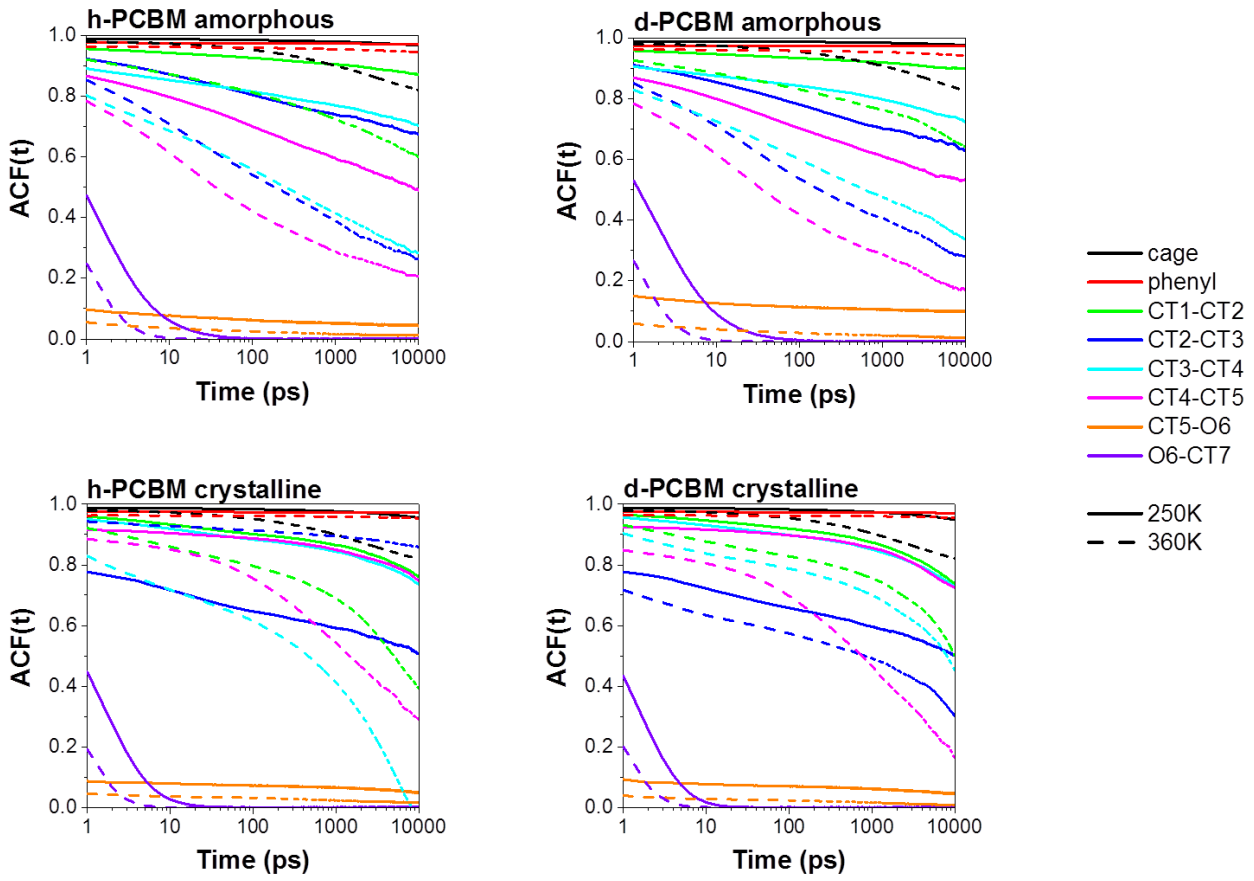

Figure S7. Autocorrelation functions of the different degrees of freedom of amorphous and crystalline h-PCBM and d-PCBM. The autocorrelation functions have been corrected for the stiffness of the degrees of freedom using S_D^2.

Table S6. Relaxation times of the different degrees of freedom of amorphous and crystalline h-PCBM and d-PCBM.

	h-PCBM				d-PCBM			
	amorphous		crystalline		amorphous		crytalline	
	250K	360K	250K	360K	250K	360K	250K	360K
cage	_	_	_	_	_	_	_	_
phenyl	_	_	_	_	_	_	_	_
CT1-CT2	_	_	_	_	_	_	_	_
CT2-CT3	_	1340 ps	_	_	_	2015 ps	_	6287 ps
CT3-CT4	_	2248 ps	_	1376 ps	_	6339 ps	_	15162 ps
CT4-CT5	_	233 ps	_	5203 ps	_	202 ps	_	2225 ps
CT5-O6	_	_	_	_	_	_	_	_
O6-CT7	2 ps	< 1 ps	2 ps	< 1 ps	3 ps	< 1 ps	2 ps	< 1 ps

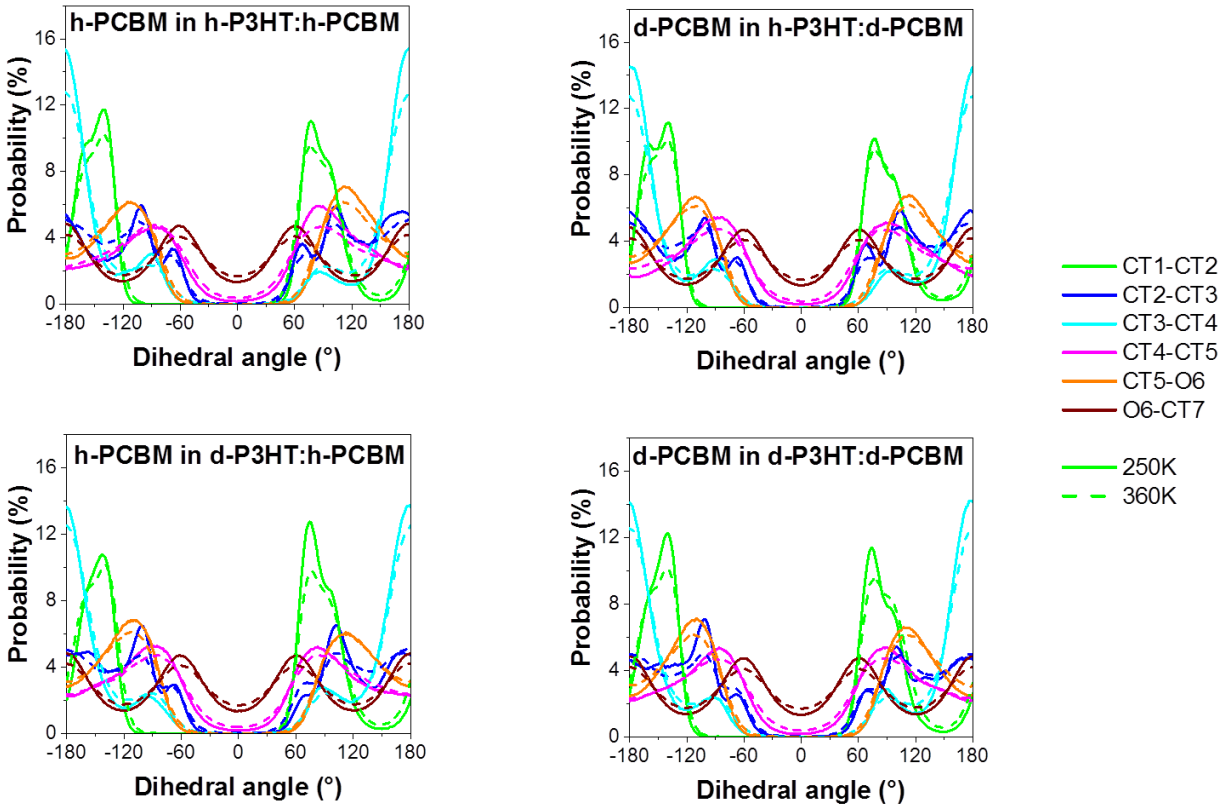

Figure S8. Dihedral distribution of the different degrees of freedom of h-PCBM and d-PCBM blended with h-P3HT and d-P3HT.

Table S7. Dihedral parameter S_D^2 of the different degrees of freedom of h-PCBM and d-PCBM blended with h-P3HT and d-P3HT.

	h-PCBM				d-PCBM			
in	h-P3HT:h-PCBM		d-P3HT:h-PCBM		h-P3HT:d-PCBM		d-P3HT:d-PCBM	
	250K	360K	250K	360K	250K	360K	250K	360K
CT1-CT2	0.219	0.213	0.201	0.210	0.218	0.218	0.188	0.216
CT2-CT3	0.168	0.174	0.189	0.176	0.179	0.175	0.187	0.173
CT3-CT4	0.552	0.501	0.523	0.490	0.542	0.502	0.540	0.497
CT4-CT5	0.042	0.028	0.033	0.029	0.029	0.028	0.036	0.027
CT5-O6	0.235	0.216	0.224	0.219	0.224	0.117	0.208	0.215
O6-CT7	0.000	0.000	0.000	0.000	0.000	0.000	0.000	0.000

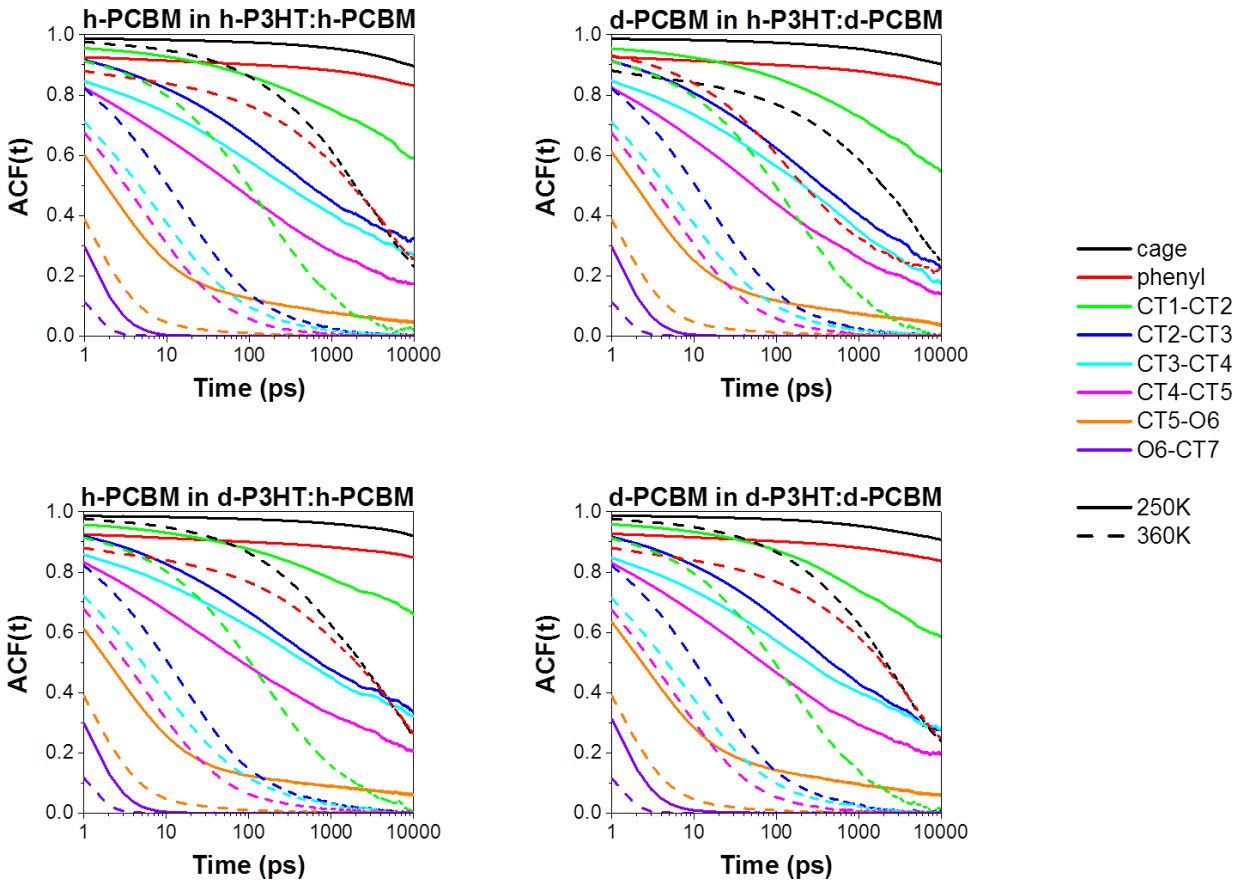

Figure S9. Autocorrelation functions of the different degrees of freedom of h-PCBM and d-PCBM blended with h-P3HT and d-P3HT. The autocorrelation functions have been corrected for the stiffness of the degrees of freedom using S_D^2.

Table S8. Relaxation times of the different degrees of freedom of h-PCBM and d-PCBM blended with h-P3HT and d-P3HT.

	h-PCBM				d-PCBM			
in	h-P3HT:h-PCBM		d-P3HT:h-PCBM		h-P3HT:d-PCBM		d-P3HT:d-PCBM	
	250K	360K	250K	360K	250K	360K	250K	360K
cage	_	4256 ps	_	5154 ps	_	4590 ps	_	4354 ps
phenyl	_	4508 ps	_	5160 ps	_	4682 ps	_	4416 ps
CT1-CT2	_	199 ps	_	224 ps	_	205 ps	_	200 ps
CT2-CT3	3406 ps	22 ps	6792 ps	22 ps	1501 ps	22 ps	2353 ps	22 ps
CT3-CT4	1731 ps	11 ps	4441 ps	12 ps	835 ps	11 ps	1846 ps	11 ps
CT4-CT5	301 ps	7 ps	519 ps	8 ps	224 ps	7 ps	321 ps	7 ps
CT5-O6	4 ps	2 ps	5 ps	2 ps	5 ps	2 ps	6 ps	2 ps
O6-CT7	< 1 ps	< 1 ps	< 1 ps	< 1 ps	< 1 ps	< 1 ps	< 1 ps	< 1 ps

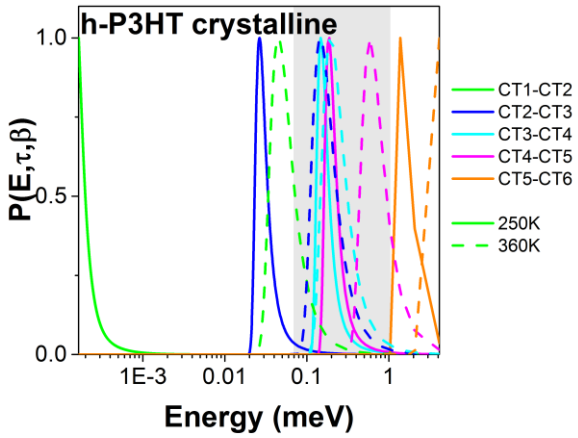

Figure S10. Simulated probability distribution functions $P(E,\tau,\beta)$ of the relaxation times of different degrees of freedom as a function of energy for crystalline h-P3HT at 250K and 360K. The grey area represents the accessible instrumental energy window on the IN6 spectrometer.[16]

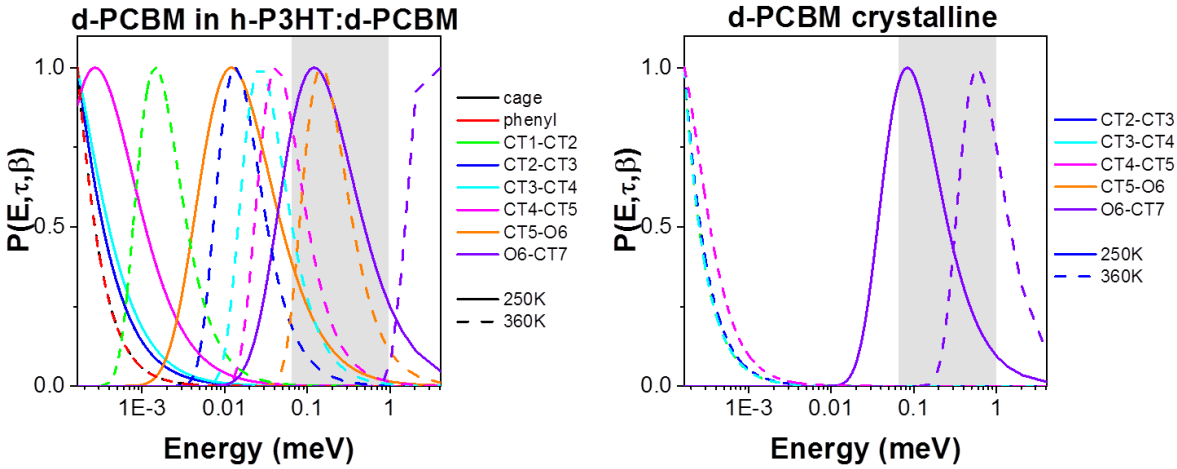

Figure S11. Simulated probability distribution functions $P(E,\tau,\beta)$ of the relaxation times of different degrees of freedom as a function of energy for d-PCBM in h-P3HT:d-PCBM and crystalline d-PCBM at 250K and 360K. The grey area represents the accessible instrumental energy window on the IN6 spectrometer.[16]

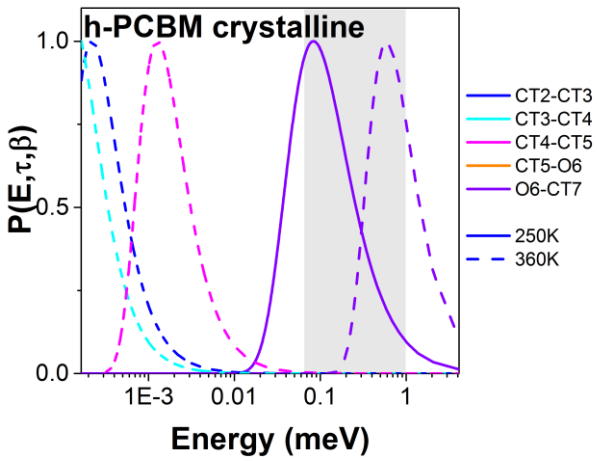

Figure S12. Simulated probability distribution functions $P(E,\tau,\beta)$ of the relaxation times of different degrees of freedom as a function of energy for crystalline h-PCBM at 250K and 360K. The grey area represents the accessible instrumental energy window on the IN6 spectrometer.[16]

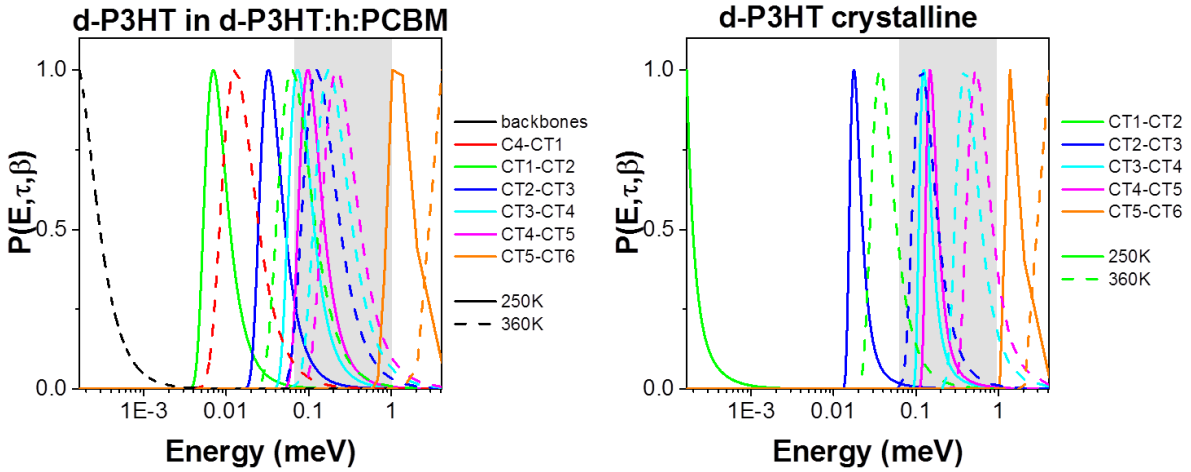

Figure S13. Simulated probability distribution functions $P(E,\tau,\beta)$ of the relaxation times of different degrees of freedom as a function of energy for d-P3HT in d-P3HT:h-PCBM at 250K and 360K. The grey area represents the accessible instrumental energy window on the IN6 spectrometer.[16]

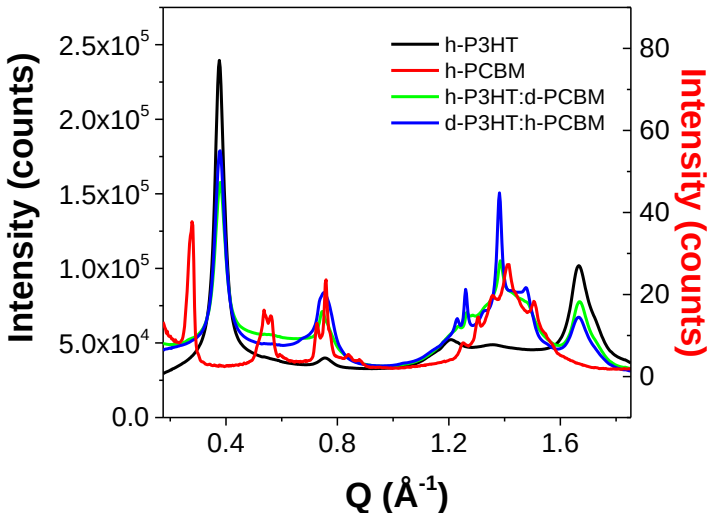

Figure S14. GIWAXS data taken in transmission for h-P3HT, h-PCBM, h-P3HT:d-PCBM and d-P3HT:h-PCBM. Note that h-PCBM was spin coated on Silicon substrate while the three other samples were hot pressed.[16]

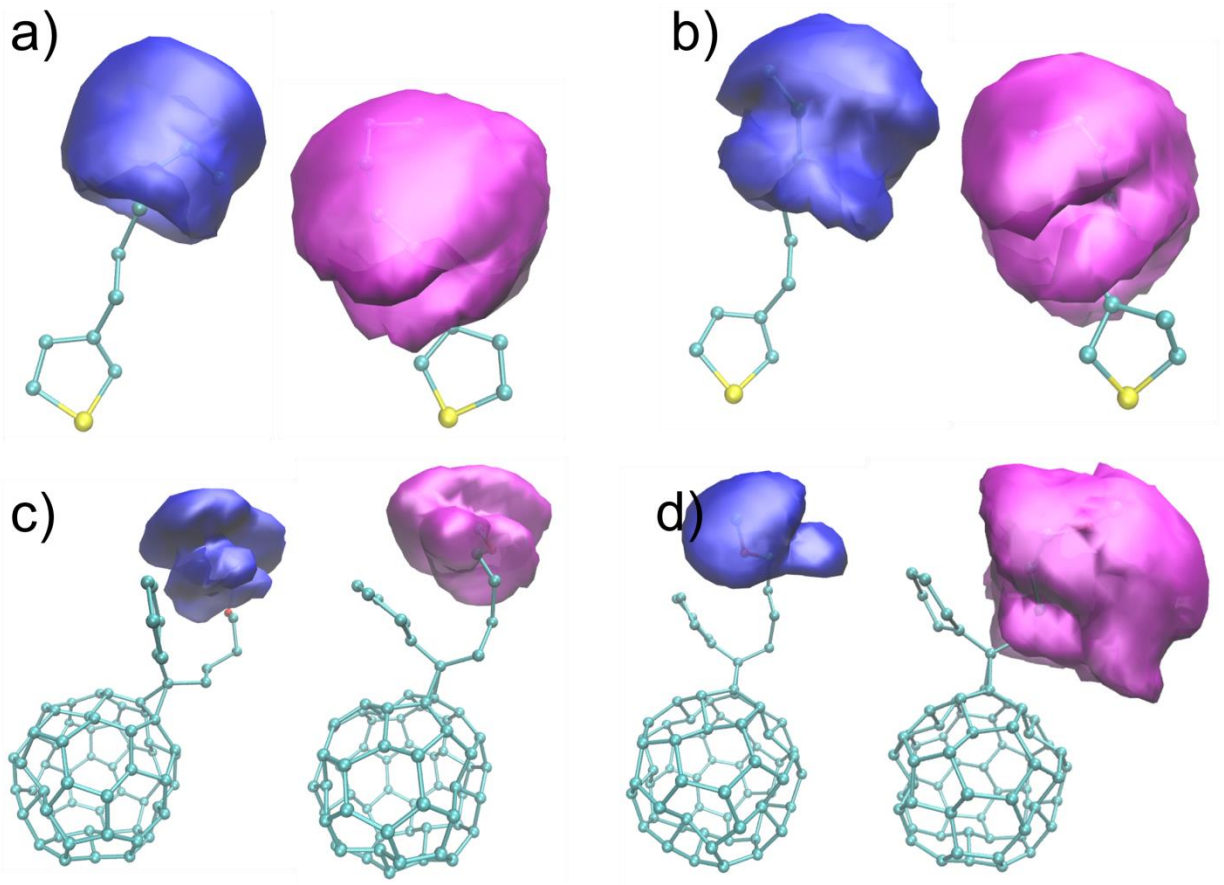

Figure S15. Spatial distribution functions of the degrees of freedom captured within the accessible instrumental energy window of IN6[16] for (a) neat h-P3HT and (b) blended with d-PCBM and (c) neat h-PCBM and (d) blended with d-P3HT at 250K (blue) and 360K (magenta).

1. Moreno M, Casalegno M, Raos G, Meille S V, Po R. Molecular modeling of crystalline alkylthiophene oligomers and polymers. *J. Phys. Chem. B* 2010;114(4):1591-602. doi:10.1021/jp9106124.

2. Darling SB, Sternberg M. Importance of side chains and backbone length in defect modeling of poly(3-alkylthiophenes). *J. Phys. Chem. B* 2009;113(18):6215-8.

doi:10.1021/jp808045j.

3. Cheung DL, Troisi A. Theoretical Study of the Organic Photovoltaic Electron Acceptor PCBM: Morphology, Electronic Structure, and Charge Localization †. *J. Phys. Chem. C* 2010;114(48):20479-20488. doi:10.1021/jp1049167.

4. Berendsen HJC, van der Spoel D, van Drunen R. GROMACS: A message-passing parallel molecular dynamics implementation. *Comput. Phys. Commun.* 1995;91(1):43-56. doi:10.1016/0010-4655(95)00042-E.

5. Van Der Spoel D, Lindahl E, Hess B, Groenhof G, Mark AE, Berendsen HJC. GROMACS: Fast, flexible, and free. *J. Comput. Chem.* 2005;26(16):1701-1718. doi:10.1002/jcc.20291.

6. Hess* B, Kutzner C, Spoel D van der, Lindahl E. GROMACS 4: Algorithms for Highly Efficient, Load-Balanced, and Scalable Molecular Simulation. 2008. doi:10.1021/CT700301Q.

7. Bussi G, Donadio D, Parrinello M. Canonical sampling through velocity rescaling. *J. Chem. Phys.* 2007;126(1):14101. doi:10.1063/1.2408420.

8. Martínez L, Andrade R, Birgin EG, Martínez JM. PACKMOL: A package for building initial configurations for molecular dynamics simulations. *J. Comput. Chem.* 2009;30(13):2157-2164. doi:10.1002/jcc.21224.

9. Guilbert AAY, Urbina A, Abad J, et al. Temperature-Dependent Dynamics of Polyalkylthiophene Conjugated Polymers: A Combined Neutron Scattering and

Simulation Study. *Chem. Mater.* 2015;27(22):7652-7661. doi:10.1021/acs.chemmater.5b03001.

10. Kayunkid N, Uttiya S, Brinkmann M. Structural Model of Regioregular Poly(3-hexylthiophene) Obtained by Electron Diffraction Analysis. *Macromolecules* 2010;43(11):4961-4967. doi:10.1021/ma100551m.

11. Casalegno M, Zanardi S, Frigerio F, et al. Solvent-free phenyl-C61-butyric acid methyl ester (PCBM) from clathrates: insights for organic photovoltaics from crystal structures and molecular dynamics. *Chem. Commun.* 2013;49(40):4525. doi:10.1039/c3cc40863a.

12. Schlitter J. Estimation of absolute and relative entropies of macromolecules using the covariance matrix. *Chem. Phys. Lett.* 1993;215(6):617-621. doi:10.1016/0009-2614(93)89366-P.

13. Lipari G, Szabo A. Model-free approach to the interpretation of nuclear magnetic resonance relaxation in macromolecules. 1. Theory and range of validity. *J. Am. Chem. Soc.* 1982;104(17):4546-4559. doi:10.1021/ja00381a009.

14. Van Der Spoel D, Berendsen HJC. Molecular Dynamics Simulations of Leu-Enkephalin in Water and DMSO. *Biophys. J.* 1997;72.

15. Berberan-Santos MN, Bodunov EN, Valeur B. Mathematical functions for the analysis of luminescence decays with underlying distributions 1. Kohlrausch decay function (stretched exponential). *Chem. Phys.* 2005;315(1-2):171-182. doi:10.1016/j.chemphys.2005.04.006.

16. Guilbert AAY, Zbiri M, Jenart MVC, Nielsen CB, Nelson J. New Insights into the Molecular Dynamics of P3HT:PCBM Bulk Heterojunction: A Time-of-Flight Quasi-Elastic Neutron Scattering Study. *J. Phys. Chem. Lett.* 2016;7(12):2252-2257. doi:10.1021/acs.jpclett.6b00537.